Astronomy & Astrophysics manuscript no. 1454 March 20, 2022
(DOI: will be inserted by hand later)

arXiv:astro-ph/0408126v1 6 Aug 2004

Late-type Giant Variables in NGC 6522, LMC and SMC How do they differ?

M. Schultheis[1,2], I.S. Glass[3], and M.-R. Cioni[4]

[1] CNRS UMR 6091, Observatoire de Besançon, BP1615, F-25010 Besançon Cedex France
[2] CNRS UMR 7095, Institut d'Astrophysique de Paris, 98bis, bld. Arago, 75014 Paris, France
[3] South African Astronomical Observatory, P,O. Box 9, Observatory 7935, South Africa
[4] European Southern Observatory, Karl-Schwarschild-Str. 2, 85748 Garching bei München, Germany

Received .... / Accepted .. ..

Abstract. Complete samples of 2MASS stars in three fields of differing metallicities (and possibly differing age distributions) have been extracted and cross-correlated with MACHO and ISO data to determine their variability and mass-loss properties.
In each M_K histogram a fall-off in numbers is seen above the tip of the RGB. The luminosity of the tip increases with metallicity as does the average $(J-K)_0$ at a given M_{K_0}. These quantities have been compared with the data for galactic globular clusters obtained by Ferraro et al. (2000). In the $J-H$, $H-K$ colour-colour diagrams, the increasing proportion of stars with high $H-K$ values is conspicuous at lower metallicities. This is well-known to result from the increasing proportion of carbon stars.
All three fields contain similar types of variables, mainly short-period (usually tens of days), Mira like (long-period, large amplitude) and double-period (having both long and short periods). The proportion of stars that vary decreases at lower metallicities and the minimum period associated with a given amplitude gets longer. Various trends are seen in the K, log$P$ diagrams of each field. The Magellanic Cloud fields largely resemble each other but the Bulge field is noticeably different. The stars that follow the 'A' K, log P relation in the Bulge hardly extend beyond $M^{\rm Tip}_{K,0}$ and the other groups also appear truncated in M_K relative to their Magellanic Cloud counterparts. In the Clouds there are many stars with periods around 200-300d that follow the 'C' or Mira relation but have relatively small amplitudes.
The mid-IR sample detected by ISOCAM during the Magellanic Cloud Mini-Survey (MCMS) appears to be reliable and complete for sources with M_K more luminous than – 7 mag, i.e., for those close to the top of the AGB. The various colour-colour and colour-magnitude diagrams reflect the increasing dominance of carbon stars at low metallicity. Mira magnitude vs log P relations exist at least up to 7μm. Mass-loss from longer-period and double-period SRVs occurs at similar rates in each field, in spite of the metallicity differences.

Key words. stars: AGB and post-AGB -stars - Magellanic Clouds - Galaxy: bulge

1. Introduction

The study of late type giant variables has been advanced greatly by the use of infrared photometry in conjunction with large-scale long-term photometric monitoring. Twenty years ago it was shown that the large-amplitude variables (Miras) in the Large Magellanic Cloud obey a period-luminosity relation (Glass and Lloyd Evans, 1981) which is particularly tight in the K–log$P$ plane (σ = 0.13) for both O- and C-rich stars (Glass et al. 1987; Feast et al. 1989). During the last few years, using the database of the MACHO gravitational lensing experiment, Wood et al (1999; see also Wood 2000) discovered that the smaller amplitude semi-regular variables of the LMC also obey period-magnitude relations, parallel to that of the Miras. Wood's work and that of Alard et al. (2001) show that the number of semiregular variables in a given population greatly exceeds that of Miras.

More recently, the nature of the K_S–log$P$ relations have been investigated with increasing thoroughness by combining the DENIS and 2MASS near-infrared sky surveys with data from the MACHO, OGLE and MOA large-scale variability projects. In particular, the SIRIUS JHK_S survey of the Magellanic Clouds, with greater sensitivity and higher resolution than its predecessors, has been used to extend the search to fainter magnitudes by Ita and collaborators (2002, 2004), with the result that the distribution of late-type variables in the K_S–log P plane is now seen to be more complex than realised at first. Ita et al. (2002) and Kiss & Bedding (2003,2004) showed that variability occurs on the upper red giant branch along sequences that extend those of the AGB to fainter mags and are slightly offset from them in log P. Cioni et al. (2000) observed that a minimum exists in the K magnitude distribution of variables in the SMC and this has been interpreted as relating to the tip of the RGB, which is metallicity dependent at K (e.g., Ita et al. 2002; Kiss & Bedding, 2004).

Send offprint requests to: mathias@obs-besancon.fr

K_S–log$P$ relations are also found among the late-type variables of the Milky Way galaxy. Glass & Schultheis (2003) have cross-correlated the DENIS and MACHO surveys of the inner Bulge field NGC 6522, whose contents are at an approximately uniform distance from the sun, and have found relations similar to those of Wood (2000).

Multi-periodic behaviour is frequently observed among the late-type variables. Most conspicuously, the lower- amplitude stars sometimes show two or more periods differing typically by factors of around 1.4, 2 or their reciprocals. A further group of stars have short periods of a few tens of days, modulated by periods about ten times longer. Wray, Eyer & Paczynski (2004) have analysed period-amplitude information, which is independent of (often unknown) distances and reddenings, for a very large sample of galactic Bulge variables from the OGLE database and have shown them to display complex multi-periodic behaviour, similar to that found in the Magellanic Clouds.

The mass-loss characteristics of late-type giants have been studied with the aid of data from the ISOCAM camera on the ISO infrared satellite, which has observed fields in NGC 6522 as part of the ISOGAL survey (Omont et al. 2003) and in the Magellanic Clouds as part of the Magellanic Cloud Mini-Survey (ISO-MCMS; Loup et al. (2004), in preparation; Cioni et al. 2001, 2003). Such mass-losing AGB stars are likely to be the most important contributors of re-cycled material to the interstellar medium in many galaxies. Cioni et al. (2001, 2003) have analysed data from the two Magellanic Clouds as seen by MACHO, DENIS and ISO-MCMS.

Alard et al. (2001), in an analysis of stars detected at 7 or 15 μm by ISOGAL in the NGC 6522 field (Glass et al. 1999), showed that they are all regular or semi-regular variables and that significant mass-loss is frequently found in red variables with periods of 70d or longer; i.e., it is not confined to Mira (by which we mean large-amplitude) variables. Using a complete spectroscopic survey of an overlapping field by Blanco (1986), it was possible to show that the variable giants belong to the later M spectral types and that the mass-losing ones in particular belong to the latest types (Glass & Schultheis 2002).

The aim of the present study has been to compare three fields in the Galaxy and the two Magellanic Clouds, as they appear in the 2MASS, MACHO and ISO databases, using the methods previously applied to NGC 6522, with the aim of seeing how the overall variability, colour, luminosity and mass-loss properties of late-type giants differ from one to another. Fields containing similar numbers of stars observed by 2MASS, MACHO and ISO have been investigated. In an analysis of DENIS data, Lebzelter, Schultheis & Melchior (2002) have already shown that the $I - J$ colours of Bulge variables have a larger range ($\sim$ 4 mag) than those in the LMC ($\sim$ 2 mag), which they attribute to the greater spread in metallicity of the Bulge compared to the LMC.

2. Sample selections

All stars with $M_{K_{S,0}} < -4.75$ were extracted from the 2MASS Catalog for three well-defined fields in the galactic bulge and the two Magellanic Clouds. This corresponds to about K_S = 9.75 in NGC 6522, 13.5 in the LMC and 13.95 in the SMC. The sizes of the fields were chosen to obtain comparable numbers of objects. Their limits are shown in Table 1. The ISO fields are considerably smaller.

Table 1. 2MASS fields in NGC 6522, LMC and SMC

field	NGC 6522	LMC	SMC
α_{min}[deg]	270.5796	80.9309	13.6301
α_{max}[deg]	271.2432	81.7392	15.6689
δ_{min}[deg]	–30.2773	–69.9094	–73.3379
δ_{max}[deg]	–29.7788	–69.6405	–72.9129
Number	1782	1809	1649
K_{lim}[mag]	9.75	13.50	13.95
Area[arcmin^2]	1032	271	905

We used the same field size for NGC 6522 as described in Alard et al. (2001) but taking the 2MASS catalog instead of DENIS. The total number of 2MASS sources is 1782 using a K_S limit of 9.75 (see Table 1). For the LMC and SMC, we have chosen fields where ISOCAM observations are available (Cioni et el. 2003). Using the final version of the 2MASS catalogue, we obtain for the SMC 1649 sources and for the LMC 1809 sources, respectively. The cut-off limits in K_S are given in Table 1.

3. Extraction of the light curves from MACHO

Counterparts for each 2MASS source in the NGC 6522, LMC and SMC fields were searched for in the MACHO database (http://www.macho.mcmaster.ca) within a typical radius of $\sim 3''$. Some 133 sources in the NGC 6522 field do not show a MACHO counterpart, while the comparable numbers are 91 in the LMC and 53 in the SMC. Occasionally, several MACHO sources were found within 2 arcsec of a 2MASS source. A unique counterpart could usually be selected on the basis of MACHO r and b value, colour, variability and proximity. Occasionally, a 2MASS source may be the sum of two or more faint non-variable MACHO sources.

Many of the missing counterparts occur because each MACHO field has one or two dead zones, corresponding to gaps between the detector chips, where cross-identifications could not be made. However, there are also cases where the MACHO tables have blank 'patches', i.e., no sources appear within 3 arcsec of the position being searched. There were 12 such positions in the LMC and 13 in the SMC. Many of the corresponding 2MASS sources were bright or 'blue' in their JHK_S colours. By means of overlays, they were found to correspond to very bright stars on the UK Schmidt IR survey plates. In many other cases, a MACHO counterpart could be found, but the data were either sparse or saturated. From their positions in the colour-colour diagrams, it is clear that sparseness of data was usually caused by saturation also, though a few of them fall among the red giants. The sparseness of the data for the latter may have resulted from crowding effects. The sparse sources are included in the near-IR colour-colour and colour-magnitude diagrams only.

4. Extraction of period information

As previously, the red and blue light curves and their frequency power spectra were plotted in batches of 20. The frequency range searched was from 0 to 0.2 cycles per day (5d to infinity in period) and the frequencies corresponding to the three most conspicuous maxima in each spectrum were derived automatically. Each light curve and power spectrum was further examined by eye. The MACHO flags were disregarded as they were often found to be too conservative. Instead, poor quality data were revealed by the light curves and the power spectra. Some data included artefacts which were noted during the visual inspection. Because of the seasonal nature of the sampling, the peaks in the power spectra were usually broader in NGC 6522 than in the Magellanic Clouds.

Multiple periodicity was found to be common in all three fields (see also Wray, Eyer & Paczynski 2004). We again made a distinction between doubly-periodic variables, which show a long period (usually several hundred days) superimposed on a short period (usually several tens of days) and stars that are multi-periodic with comparable periods (usually several tens of days).

The Fourier spectra of the doubly-periodic stars were sometimes dominated by harmonics of the (non-sinusoidal) longer period variations, so that their short periods were not always among the three highest peaks that were extracted automatically. Occasionally also there was poor agreement between the blue and red data. In the first-mentioned category, the short period could usually be found among the lesser peaks of the Fourier spectrograms and, in the more difficult cases, a visual estimate of period could be made from coherent portions of the light curves. The short and long periods were recorded together with visual estimates of their long-term average peak-to-peak amplitudes.

The stars with secondary short periods often showed more than two of them. We recorded the two most prominent short periods and the long period, if present, as well as the full amplitude of the short and long-period variations, averaged by eye from the light curves. The ratios of the short periods were plotted against the log of the dominant period as in fig. 9 of Glass & Schultheis (2003) for each field. The frequency of detectability of secondary short periods was lower in the Magellanic Clouds than in NGC 6522 but there were no obvious differences in the general character of the plots.

The Mira variable D9 in the NGC 6522 field was too bright for MACHO and has been assigned the approximate period 400d (Lloyd Evans1976) and an arbitrary *r* amplitude of 4 mag for completeness.

The few Cepheid variables present in the Magellanic Cloud data were apparent from their MACHO light curves. Only one eclipsing binary, possibly of contact type, MACHO 211.16650.11, was found, lying in the direction of the SMC.

5. Amplitudes

The full amplitude of the short (and long, if present) period variations were recorded from eye estimates, using the MACHO *r* band data or, if lacking, the *b*. In the case of multiple short periods, the overall peak-to-peak amplitude was recorded. For doubly periodic variables, both amplitudes were noted. Generally, amplitudes were categorized as 0, 0.05, 0.1, 0.15, 0.2, 0.3, 0.4 ... mag. The 0.05 category includes stars whose variability was just detectable. It is estimated that variability with peak-to-peak amplitude of ≥0.03 mag was detected.

6. Discussion: Near-IR

In what follows, we have assumed a distance modulus for the NGC 6522 field of 14.7, for the LMC 18.5 and for the SMC 18.94. The extinction values that we took were: $E_{B-V} = 0.5$ for NGC 6522, $E_{B-V} = 0.15$ for the LMC and $E_{B-V} = 0.065$ for the SMC. These were applied to the JHK_S data according to the extinction law given by Glass (1999). The plots given in this paper make use of the de-reddened absolute magnitudes for ease of comparison. It should be noted that the distance modulus of 14.7 used for the NGC 6522 field (Glass et al. 1995) is higher than that commonly accepted. It is retained here because it gives good fits to the M_{K_S}, log$P$ sequences defined from the Magellanic Cloud samples.

The stars plotted in the JHK-region diagrams are divided into the following classes: crosses: saturated and sparse stars; circles: non-variables; solid dots: small- amplitude variables; boxes: doubly-periodic stars; asterisks: large-amplitude variables. Note that doubly- periodic stars were only counted as such if the full MACHO *r* amplitude of the longer period exceeded 0.2 mag. Large-amplitude variables are those with full MACHO *r* amplitude > 1.0 mag.

6.1. Colour-magnitude diagrams

The left side of Figure 1 shows the colour-magnitude diagrams of the sources detected in MACHO and 2MASS for the NGC 6522 field, the LMC and the SMC. The densest part of each diagram is enlarged on the right.

All three fields are dominated by the giant sequence, composed of the AGB (mainly upper part) and the RGB (lower part). The most conspicuous trend is that the giant branches move blueward in $(J - K_S)_0$ colour as one progresses from the NGC 6522 to the SMC fields. A lower metallicity is known to lead to a shift of the giants towards higher temperatures in the HR diagram and thus to bluer colours. According to Kiss & Bedding(2004), the tip of the RGB occurs at $M_{K_{S,0}} = -6.48$ in the LMC and – 6.26 in the SMC. Our K histograms (fig. 2) show that the steep fall-off in numbers which occurs at this point (see also Cioni 2000) is separated by about 0.3 mag between the SMC and the LMC and by a similar amount between the LMC and the NGC 6522 field. The level of the RGB tip is shown as a dotted line in each case (fig. 1). The fall-off in the number of stars is accompanied by a noticeable decrease in average $(J - K_S)_0$ colour in the LMC and SMC.

According to the work of Ferraro et al. (2000) on galactic globular clusters,

$$M_{K_0}^{\mathrm{Tip}} = -(0.59 \pm 0.11)[\mathrm{Fe/H}] - (6.97 \pm 0.15).$$

There is a small transformation between K_S^{2MASS} and K^{SAAO}, so that, if we take the Kiss & Bedding figures and assume that the

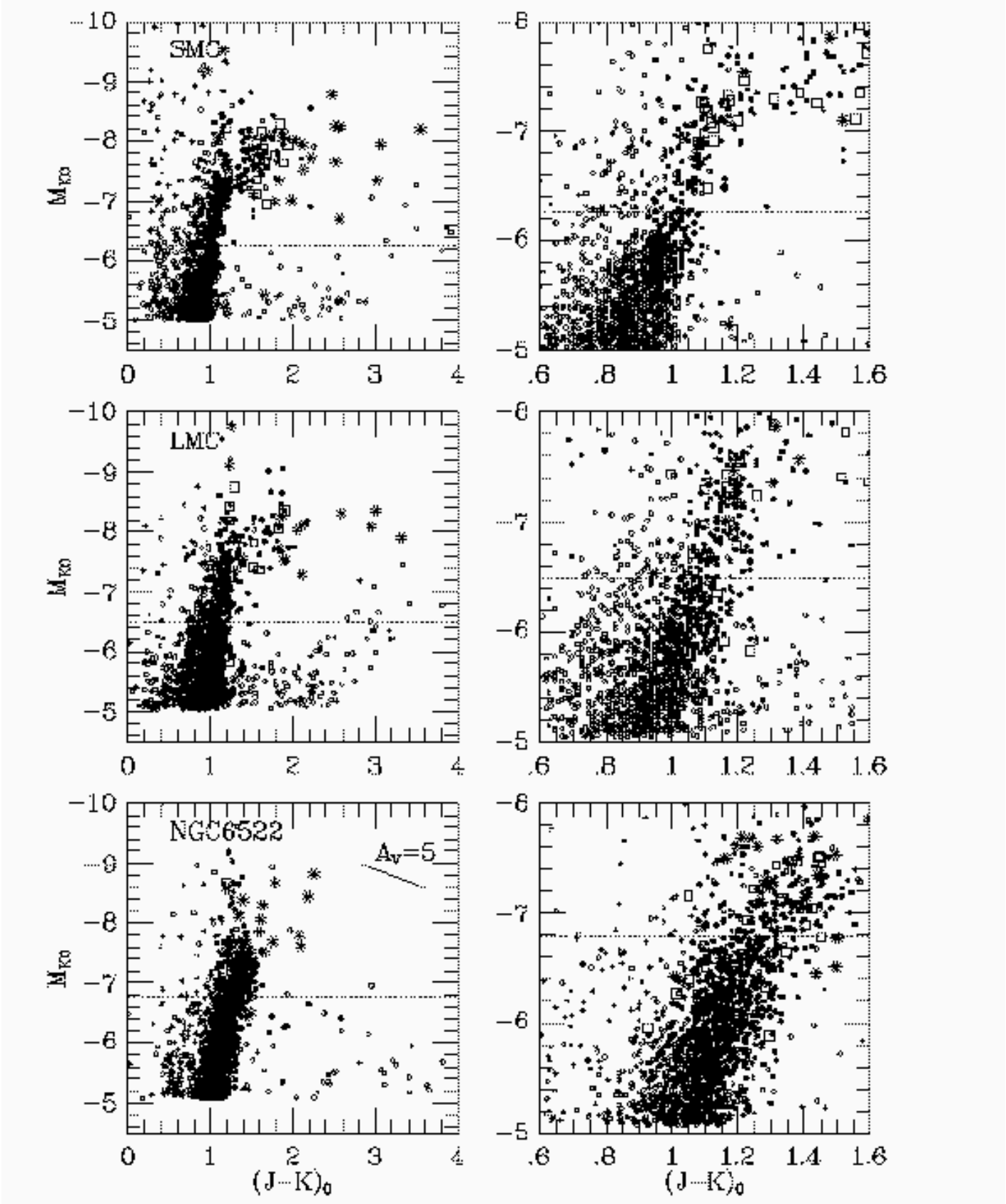


Fig. 1. *Left:* $M_{K_{S,0}}$ vs. $(J-K)_0$ diagram for the NGC 6522 field (bottom), the LMC (middle) and the SMC (top). Saturated and sparse stars are indicated as crosses, non-variable stars as open circles, semiregular variables as filled circles, doubly-periodic SRVs as open squares and large amplitude Mira variables as asterisks. *Right:* Enlargement of densest portion of diagrams. Most of the points towards the bottom right of the distributions, i.e., with $(J-K_S)_0 > 1.2-1.4$ and $M_{K_{S,0}} > -7$, are probably the result of photometric errors or crowding, since they are constant or of small amplitude (and are thus not large amplitude variables surrounded by dust shells). The dotted lines represent the estimated levels of the RGB tips.

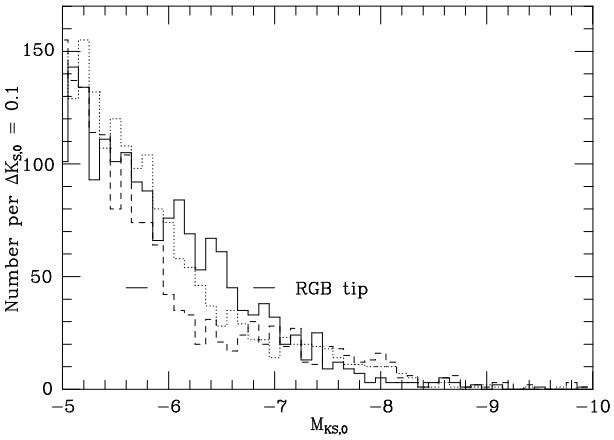


Fig. 2. Comparative histogram of $K_{S,0}$ for the three fields to show the sudden drop-off at the RGB tip. The NGC 6522 field is given by the solid line, the LMC field by the dotted line and the SMC field by the dashed line.

NGC 6522 field RGB tip is 0.3 mag brighter than that of the LMC, we obtain rather low values of the metallicities for the NGC 6522, LMC, and SMC fields of [Fe/H] = – 0.32, – 0.85 and – 1.22 respectively.

The average $(J-K)_0$ value at a given M_K is also an indicator of metallicity. We have determined this to be (for $-5.25 > M_{K_{S,0}} > -5.75$) 1.09, 0.99 and 0.89 for the NGC 6522, LMC and SMC fields respectively. To place these values on the SAAO system, for which the Ferraro et al. (2000) relation is valid, the transformation given on the 2MASS website must be applied

$$(J-K_S)_{2MASS} = (0.944 \pm 0.012)(J-K)_{SAAO} - (0.005 \pm 0.006)$$

The $(J-K)_0$ values then become 1.16, 1.05 and 0.95 on the SAAO system. Ferraro et al. (2000) give

$$(J-K)_0^{-5.5} = (0.21 \pm 0.01)[\mathrm{Fe/H}] + (1.13 \pm 0.02)$$

The metallicities according to this criterion are then 0.14, – 0.38 and – 0.86 for the NGC 6522, LMC and SMC fields, respectively. Terndrup, Frogel & Whitford (1990) found [M/H] ~0.2 from M giants in inner Bulge fields. Young ($< 10^9$ yr) populations in the Large Magellanic Cloud have [Fe/H] ~ – 0.2 and in the Small Cloud ~ – 0.5, but for older populations these figures can be as much as 1 dex smaller (Feast, 1989). The metallicity values derived from the RGB tip magnitudes are lower by about 0.4. A discussion of the uncertainties in these relations is given by Ferraro et al. (2000). The present results, though not consistent in absolute metallicity, at least agree that metallicities differ by about 0.4 to 0.5 dex between the Bulge and the LMC and between the LMC and SMC fields. It can also be that age affects the stars at the tip of the RGB differently from those at $M_K = -5.5$.

6.1.1. Relation to theoretical isochrones

Differences in tip RGB K luminosities due to age and metallicity can be estimated using theoretical isochrones from Girardi et al. (2000). Consider first the differences in $M_{K_S}^{\mathrm{Tip}}$ for two populations of *fixed metallicity* that are about 3 and 10 Gyr old. These amount to 0.16, 0.23 and 0.27 mag for Z = 0.004, 0.008, and 0.019, respectively, approximately corresponding to the average metallicities of the SMC, LMC and NGC6522. Clearly, differences due to age are stronger in a metal-rich population.

If we compare $M_{K_S}^{\mathrm{Tip}}$ for populations with *fixed ages* of 10 Gyr but differing metallicities we find the difference in $M_{K_S}^{\mathrm{Tip}}$ between Z=0.004 and Z=0.008 is 0.32 mag and the difference between Z=0.008 and Z=0.019 is 0.19 mag. For 3 Gyr old populations, these figures become 0.25 and 0.15 mags. Differences due to metallicity are thus somewhat greater for an older population.

It is believed that each of these galaxies contains a composite stellar population and therefore the observed 0.3 mag difference in the tip of the RGB is most probably the result of both age and metallicity effects. Since the Clouds are closely related and it is possible that their RGB populations have the same age, or the same mixture of ages, may be that the ≥0.3 mag difference can be explained by a metallicity effect alone. However, more realistically, within each Magellanic Cloud a spread in metallicity of order 0.75 dex is likely to be present (Cioni & Habing 2003a) or at least to have been present at the time their AGB stars were formed.

6.1.2. Further comments on the colour-magnitude diagrams

There are increasing numbers of stars redward of the top of the AGB at $M_{K_{S,0}} \sim -8$ as lower metallicities are approached. The reddest of these stars in the NGC 6522 field are O-rich Mira variables, whereas in the Magellanic Clouds they may also be C-rich Miras. However, it is clear that there are many low-amplitude and double-period Magellanic Cloud variables with elevated $(J-K_S)_0$ that have no counterparts in the NGC 6522 field. These are probably C-rich. It is well-known (Lloyd Evans 1988) that carbon stars are more abundant among large amplitude variables in the SMC than the LMC.

It is also curious that there are no doubly-periodic variables fainter than the red giant tip in the SMC field, whereas there are three in the LMC and many in NGC 6522.

There are considerable populations of non-variable stars around 0.3 mag blueward of the giants in the Magellanic Cloud fields, though not in NGC 6522. Many of these have $(J-K_S)_0 < 0.5$ and are most likely galactic foreground objects. There is a higher proportion of galactic foreground stars in the LMC ($(J-K_S)_0 \sim 0.7$), than in the SMC. (see Nikolaev & Weinberg 2002).

6.2. Colour-colour diagrams

Figure 3 shows the $(J-H)_0$ vs. $(H-K_S)_0$ colour-colour diagram of the MACHO variables.

Especially the LMC diagram contains a large number of spurious points to the right of the concentrated area and some others directly above it. These are suspected to arise from errors in the 2MASS photometry and errors in the cross-

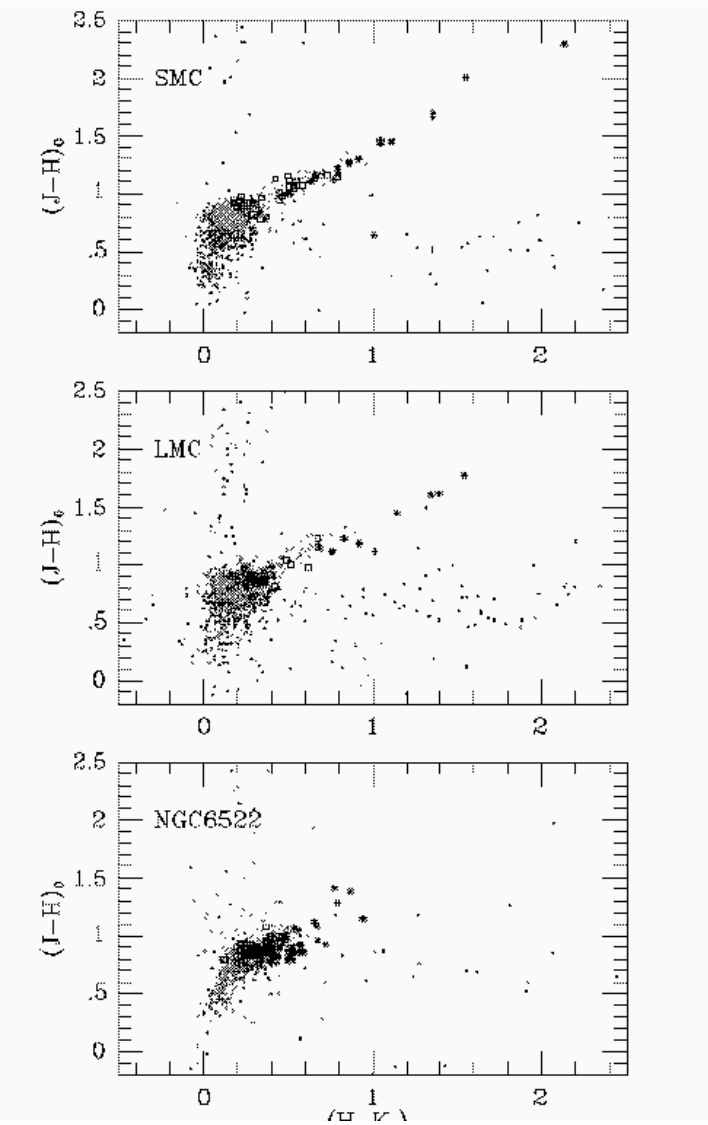


Fig. 3. $(H-K_S)_0$ vs. $(J-H)_0$ colour-colour diagram for the NGC 6522 field (bottom), the LMC (middle) and the SMC (upper). Non-variable and saturated stars are indicated by black dots, semiregular variables by grey, doubly–periodic SRVs by open squares and Mira variables by asterisks. Some features can be seen more clearly on a colour version of this figure, available at ...

identifications between bands. Similar effects occur in the DENIS data. This diagram can be seen in colour on the ... web site, with constant stars coded blue, saturated stars magenta, small-amplitude variables green, doubly-periodic cyan and Miras red. The constant stars (many of them in the foreground) extend the concentrated area in the direction of bluer and less luminous stars (see the colour version for a clearer picture).

While the colour-colour diagrams of the LMC and SMC look rather similar, the stars in the NGC 6522 field have a smaller overall range in $(J-H)_0$ and $(H-K_S)_0$ because of the red colour of the many carbon stars in the LMC and SMC which do not occur in the Bulge. The $J-H$ and $H-K$ colours are sensitive to metallicity and atmospheric extension (Bessell et al. 1996).

The doubly-periodic stars in the Magellanic Clouds are among the reddest of the small-amplitude variables (even their longer periods rarely exceed 1.0 mag). They can be redder than their counterparts in NGC 6522. At least some of them will be carbon stars. However, Groenewegen (2004) has cautioned against deciding on carbon- vs oxygen-richness on near-IR colours alone.

6.3. Magnitude distributions

Stars whose peak-to-peak amplitudes were lower than 0.03 mag in *r* were generally not detectable as variables. This limit is somewhat subjective and depends on the quality and quantity of the data for the individual objects, neither of which are absolutely uniform. The possibility exists that some of the objects classified as non-variable may, in fact, be variables of very small amplitude. The dependence of variability on spectral type was discussed by Glass & Schultheis (2002).

Figure 4 shows the distributions of absolute $K_{S,0}$ magnitude for the variable and non-variable stars. Indicated are also the locations of the tips of the RGB as discussed previously. It is clear that the variable stars on the AGB dominate the non-variables by far. While this is also true for the SMC and LMC, the ratio of variables to non-variables is much higher in the NGC 6522 field than in the LMC and the SMC. This tendency remains dominant for the Bulge up to about $M_{K_{S,0}} \sim -5$ (see Fig. 4) which is presumed to be the completeness limit for detecting variable stars. For the LMC and SMC the characteristics of 2MASS cause this limit to be about $M_{K_{S,0}} \sim -6$. Thus the proportion of variable stars beyond the tip of the RGB decreases as we go downwards in metallicity from the NGC 6522 field to the SMC field.

A further important characteristic is that the proportion of luminous AGB stars with $M_{K_{S,0}} < -7.5$ increases with decreasing metallicity. It will be seen later (section 7) that these constitute most of the stars detected by ISO in the Magellanic Clouds.

6.4. Period-$M_{K_{S,0}}$ relations

Figure 5 shows the $M_{K_{S,0}}$, log *P* diagram for the three fields. The Magellanic Cloud fields show a number of clearly separated sequences, but in the NGC 6522 field they overlap considerably because of the depth of the galactic bulge along the line-of-sight.

Diagrams of this kind with much larger numbers of stars have been produced for the Magellanic Clouds by other authors (e.g., Ita et al. 2004, Kiss & Bedding 2003, 2004) and some of the subtler aspects of the distributions are better seen in their work.

The scatter about relation C (the Miras) is higher than in previous work (e.g., Glass et al. 1995) because these variables have large amplitudes and only single-epoch observations at K_S are used here.

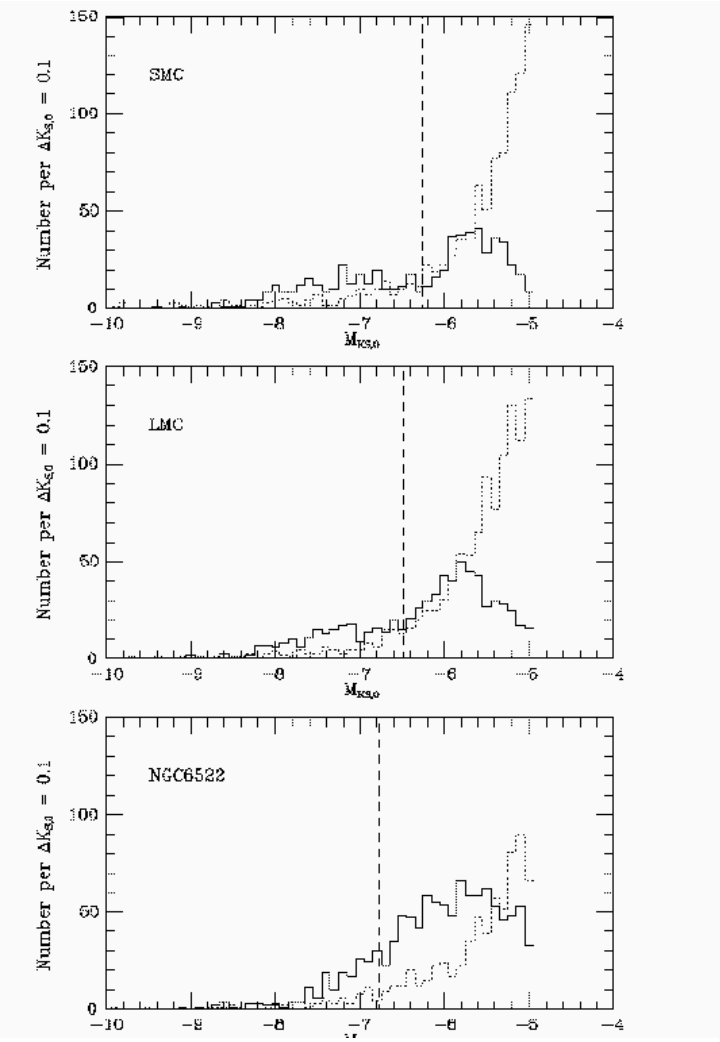


Fig. 4. Histogram of $K_{S,0}$ for variable stars (full line) and non-variable stars (dotted line). The dashed lines indicate approximately the locations of the tips of the RGBs (see text).

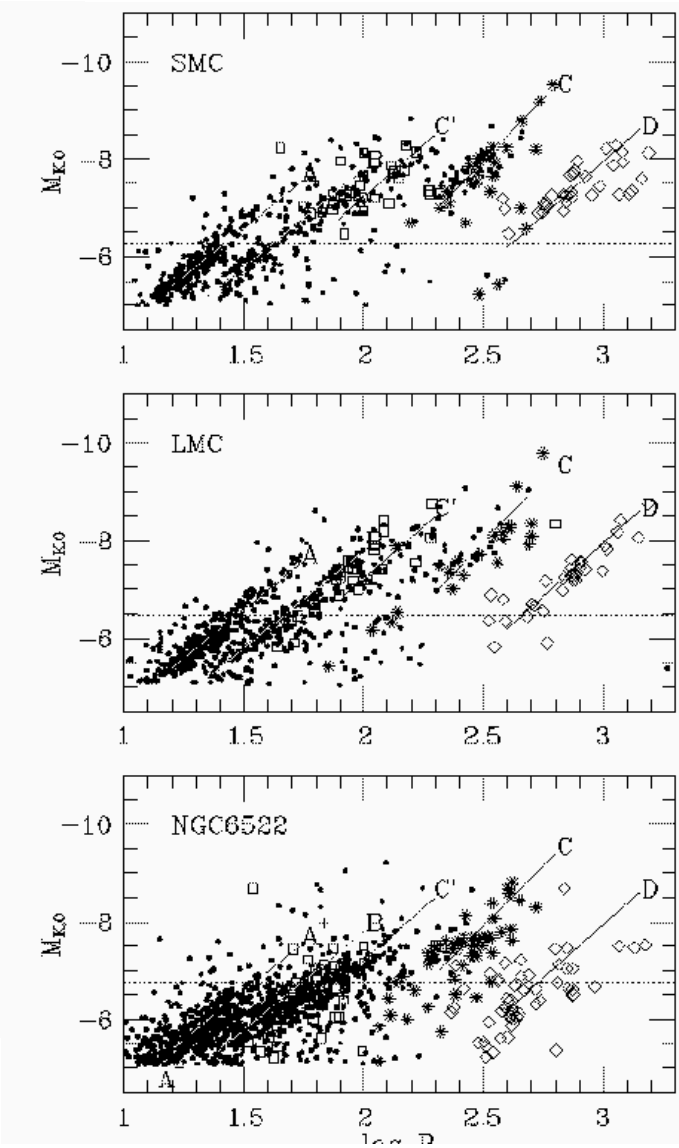


Fig. 5. log P vs. $M_{K_{S,0}}$ relation for the NGC 6522 field (bottom), the LMC (middle) and the SMC (top). Small amplitude variables are indicated by filled circles, doubly-periodic SRVs by open squares (short periods) and diamonds (long periods) and Mira variables by asterisks. The straight lines are eye fits to the LMC sequences. The level of the top of the RGB is indicated by a dotted line.

The LMC diagram has been fitted by eye with a number of lines that indicate the positions and extents of the discernable sequences. These lines have been copied onto the other fields to aid in intercomparisons. Ita et al. (2004) (Fig 1) gives outline boxes for the sequences in the two Magellanic Clouds. To the original ABCD of Wood et al. (2000) they have added a sequence C′, which we see clearly in both these fields, though they do not separate it from their B^+ in the SMC. They further divide Wood's A and B sequences at the tip of the RGB into separate ones (A^-, A^+, B^-, B^+). We have divided only the A sequence in our diagram.

The slopes of the sequences seem to be very similar between the two Magellanic Clouds and are probably also compatible with the NGC 6522 field, though here the scatter is too large for a strict comparison to be made.

We have indicated by dotted lines the approximate locations of the RGB tips as discussed previously.

The short periods of the double-period variables appear on the B and C′ sequences, but not on A or C. Their long periods appear along a sequence of their own (D). The nature of the long-period variations is not yet understood.

There are strong differences in this diagram between the galactic and Magellanic Cloud samples. In general, the Magellanic Cloud sequences extend to brighter absolute magnitudes than the NGC 6522 field and have higher proportions of luminous variables. Although this conclusion may not be statistically firm for the C (Mira) sequence, it is very clear in the A, B and C′. In fact, the A sequence in NGC 6522 may not even extend above the RGB limit. Kiss & Bedding (2003) show that

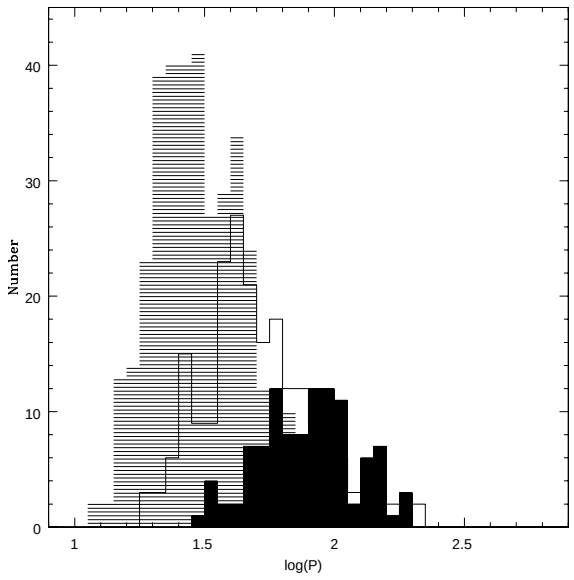


Fig. 6. Period distribution of small-amplitude variable stars with 0.05 < A < 0.2 for NGC6522 (shaded histogram), the LMC (empty histogram) and the SMC (filled histogram).

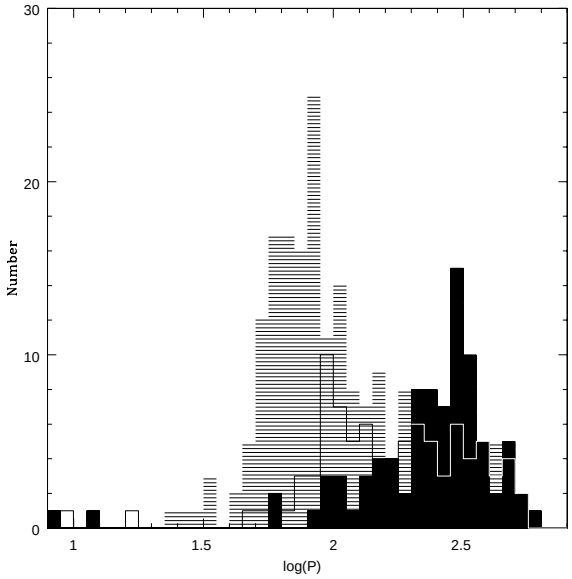


Fig. 7. Period distribution of large-amplitude variable stars with A > 0.2 for NGC6522 (shaded histograms), LMC (empty histogram) and the SMC (filled histogram).

stars on these extensions frequently have red $J - K_S$ colours, which makes them likely to be C-rich.

At lower metallicities, the lower end of the C sequence, normally associated with Miras, is populated by increasing numbers of small-amplitude variables. These are numerous in the SMC and very rare in NGC 6522.

6.5. Amplitude distributions

Figure 6 shows the period distribution for the small-amplitude (< 0.2 mag) and Fig. 7 that for the large-amplitude variables in the three different fields. They show that the amplitudes (both small and large) decrease progressively from the NGC 6522 to the SMC fields. A longer period is reached at a given amplitude as the metallicity decreases, or alternatively a given amplitude is attained at a longer period when the metallicity is low. For example, stars with amplitude smaller than 0.2 mag show their peak at log $P \sim 1.35$ in NGC 6522, at log $P \sim 1.6$ in the LMC and at log $P \sim 1.9$ in the SMC.

The general distribution of larger-amplitude variables seems to be very similar in the Bulge, LMC and SMC. For log P up to ∼2.0 in the galaxy and ∼2.3 in the Clouds, the amplitudes stay small (< 0.2 mag) before increasing dramatically to $1 < A < 5$ mag (see Fig. 8). However, the fraction of all (including the large-amplitude) variables is smaller for metal-poorer environments. Indeed, one expects that the visual amplitudes will in general be smaller for lower metallicity which makes the bands of highly sensitive molecules like TiO (Reid & Goldston 2002) weaker. This would favour small amplitude variability in metal poor environments and explain the smaller fraction of large amplitude objects in the SMC compared to the LMC and the galactic Bulge. This picture is also consistent with the complete lack of Miras in metal-poor globular clusters (Frogel & Whitelock 1998). It is also the case that stars traditionally classified as carbon Miras in the Large Magellanic Cloud tend to have smaller amplitudes than their M-type counterparts (Glass & Lloyd Evans 2003).

6.6. Colour, log P diagrams

Fig. 9 shows the $(J - K)_0$, log P diagram for each field. The thickness of the $(J - K)_0$ distribution of the short-period variables (up to 100d) is highest in the NGC 6522 field. The Magellanic Cloud fields show increasing numbers of carbon SRVs at log$P$ > 2.0. These have $(J - K_S) \geq 1.4$ in the Magellanic Clouds; this colour can be used as a diagnostic tool. The $(J - K_S)_0$ colour of some Miras is lower than that of SRVs of similar period, probably because of the onset of water-vapour absorption which, unlike CO, is contained in the K_S bandpass and thus is more likely to affect it than the regular K bandpass.

7. Discussion: Mid-IR

7.1. ISO observations

Parts (see Table 2) of our three fields were observed at mid-IR wavelengths by the ISOCAM camera on ISO. The fields in the LMC and SMC formed part of the Magellanic Cloud Mini-Survey (Loup et al. (2004), in preparation), which used the LW2 (or 7μ, range 5–8.5 μm, centre wavelength 6.7μm) and the LW10 (12μm, range 8–15 μm, centre 12.0μm) filters.

The NGC 6522 Baade's Window was observed as a fiducial field during the the ISOGAL survey of the galactic plane and inner Bulge (Omont et al. 2003), using the same 7μm filter but a different longer wavelength one, the LW3 (or 15μm filter,

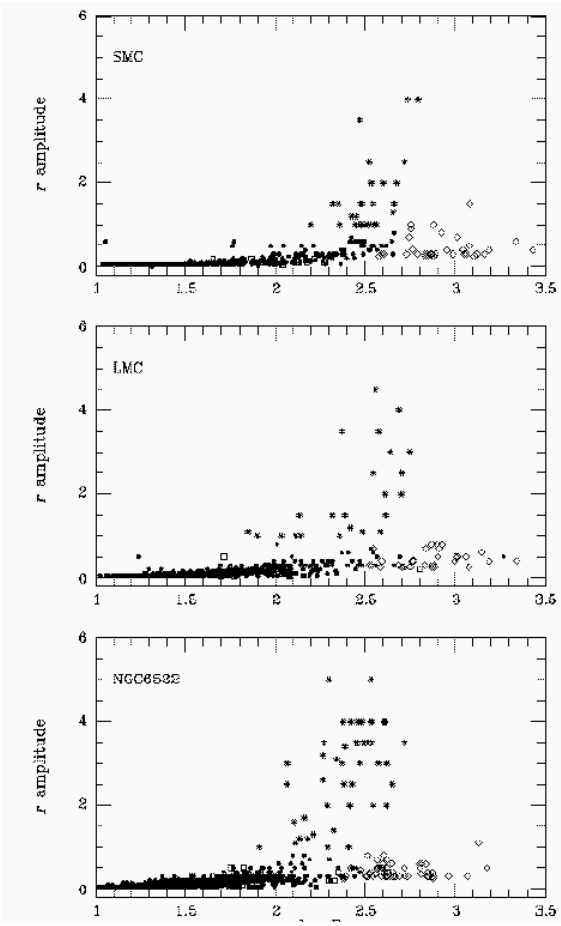


Fig. 8. General MACHO log$P$ vs. amplitude diagram for the NGC 6522 field (bottom), the LMC (middle) and the SMC (upper). Non-variable stars are indicated by crosses, semiregular variables by filled circles, doubly-periodic SRVs by open squares and Mira variables by asterisks. Large-amplitude variation occurs at a shorter period in the more metal-rich NGC 6522.

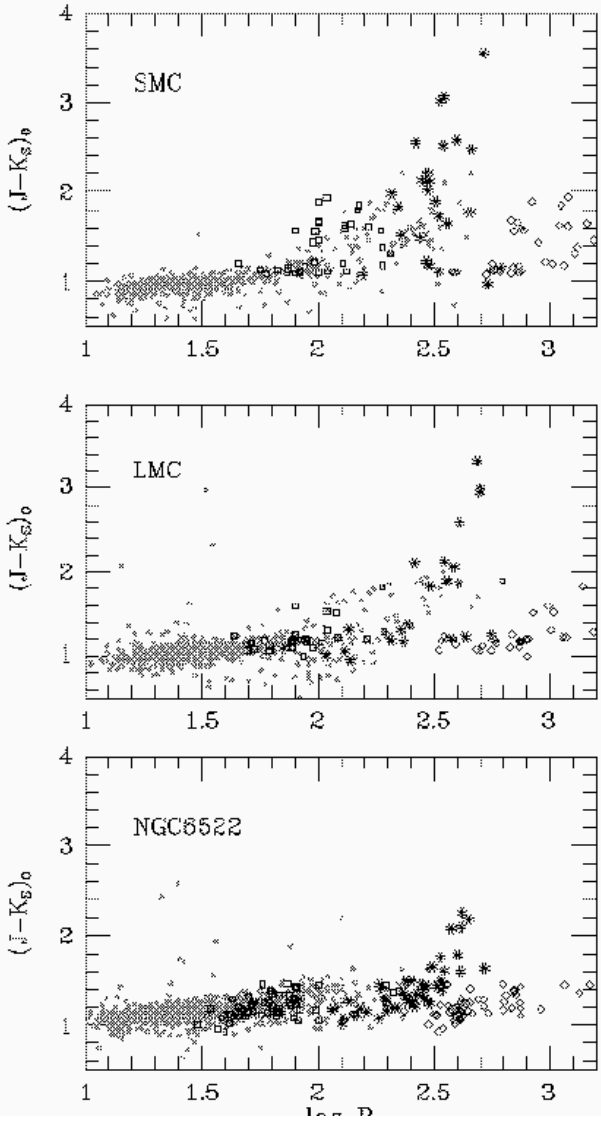


Fig. 9. $(J-K_S)_0$ vs log P diagrams. The effect of carbon stars is obvious among the SRVs with periods around 100d and longer as well as the doubly-periodic stars and the Miras.

range 12.0–18μm, centre 14.3 μm). The following conversions between flux and magnitude are used:[1]

[7] = 12.38 – 2.5log$F_{\nu,LW2}$(mJy)

[12] = 11.13 – 2.5log$F_{\nu,LW10}$(mJy)

[15] = 10.79 – 2.5log$F_{\nu,LW3}$(mJy)

No reddening corrections have been applied to the ISO data since they are small and uncertain. The observational errors in the current sample are typically ±0.14 mag at each wavelength.

It should be remembered that the ISO and 2MASS observations were not simultaneous so that the combination of near- and mid-IR data, particularly of the large-amplitude variables, may be affected.

The number of ISO detections as a function of the K magnitude is shown in Fig. 10. While the ISO detections in the LMC and SMC evidently become incomplete fainter than $M_{K_0} \sim -7$, the NGC 6522 field can be regarded as complete down to $M_{K_0} \sim -5.5$. As already pointed out by Glass & Schultheis (2002), ISO detections are complete for NGC 6522 at the tip of the RGB. For the LMC and SMC, only the most luminous AGB

[1] For [12] see Origlia et al, ApJ 571, 458, 2002.

Table 2. ISO fields in NGC 6522, LMC and SMC

field	NGC 6522	LMC	SMC1	SMC2
α_{min}[deg]	270.624	80.932	13.909	14.819
α_{max}[deg]	270.961	81.718	14.755	15.615
δ_{min}[deg]	-30.118	-69.907	-73.246	-73.167
δ_{max}[deg]	-29.834	-69.641	-73.006	-72.929
Number[1]	261	334	227 (total)	
Area[arcmin^2]	225	261	411 (total)	

[1]Number of ISO sources in field with 2MASS counterparts but irrespective of MACHO cross-identifications.

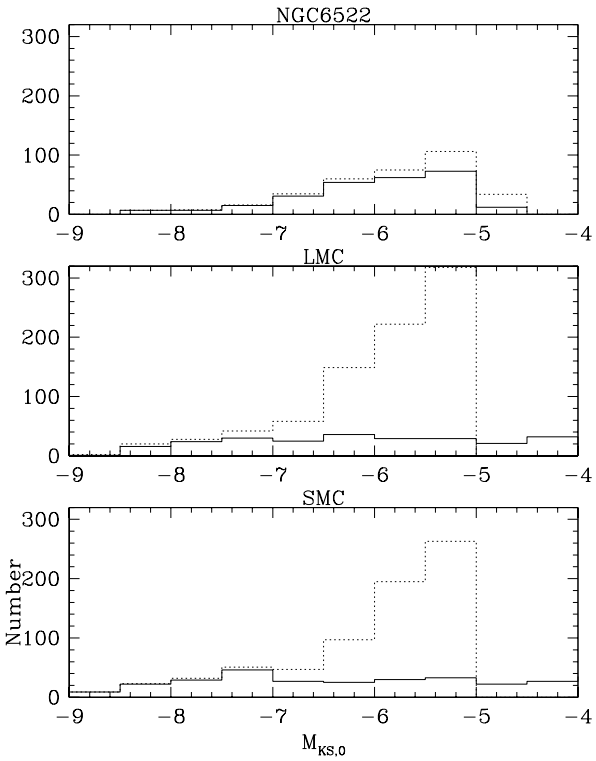


Fig. 10. Histogram of $M_{K_{S,0}}$ for stars associated with ISO sources (straight line) and not associated (dotted line). ISO identifications with 2MASS sources are likely to be unreliable fainter than $M_{K_{S,0}}$ = –7 in the Magellanic Clouds and –5 in NC6522.

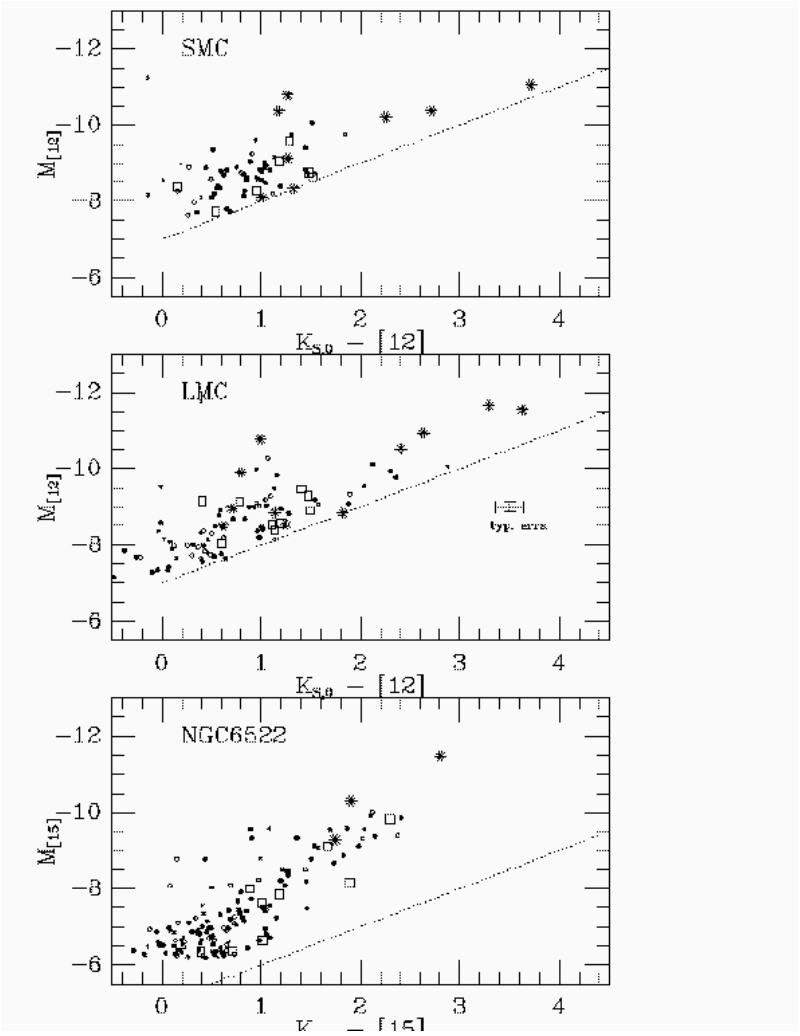


Fig. 11. [12/15] vs K – [12/15] colour-magnitude diagram. The dotted line indicates the likely limit of reliability of the 2MASS-ISO cross-correlations. Note that objects in NGC 6522 are detected to much lower luminosities than in the LMC and SMC. However, the Magellanic Clouds have a substantial population of objects around M_{12} = – 8 to – 10 and $K_{S,0}$ – [15] = 1 which is not the case in NGC 6522.

stars are complete. Many of the detected objects have ($J - K_S$) > 1.4 (fig. 1) but it will be seen that this does not necessarily imply that they are C-rich. The associations less luminous than $M_{K_0} \sim -7$ are probably by chance in most cases. They have been omitted from further discussion.

7.2. Near- to mid-IR colour-magnitude diagram

Figure 11 shows the $K_{S,0}$ – [12/15] vs. [12/15] diagram. Note that the LW10 filter which is used for the LMC and SMC is close to the IRAS 12 μm filter whereas the ISOGAL LW3 filter is centered around 15 μm. The LW10 filter includes the 9.7 μm silicate and the 11.3 μm SiC dust features. Superimposed is the approximate completeness limit in K_0, arising from 2MASS, as described above. Most, but possibly not all, of the (eliminated) points below this line are spurious ISO-2MASS associations but some could be real detections affected by thick circumstellar shells. As already discussed by Alard et al. (2001) and Glass & Schultheis (2002), the K_0 – [15] vs. [15] diagram in NGC 6522 reveals a mass-loss sequence in which the large-amplitude Mira variables are situated at the top of the diagram. This mass-loss sequence is also shown in Fig. 11 for NGC 6522.

Cioni et al. (2003) studied long-period variables detected by ISO in the SMC. They found that Mira variables have large K_S – LW10 colours, where the carbon-rich objects show on average redder colours than the oxygen-rich stars. Figure 11 shows that the diagrams for the LMC and SMC are quite different. The numbers of high mass-losing semiregular variables with ($K_{S,0}$ – [12]) > 1.5 (black dots) seem to decrease going to lower metallicities and are totally absent in the SMC. However, one has to be extremely careful concerning selection effects and small-number statistics.

7.3. Two near- to mid-IR colour-colour diagrams

7.3.1. ($H - K$) vs (K – [7])

In the near- vs mid-IR colour-colour diagram (fig. 12), the range of colours present in NGC 6522 is small compared to

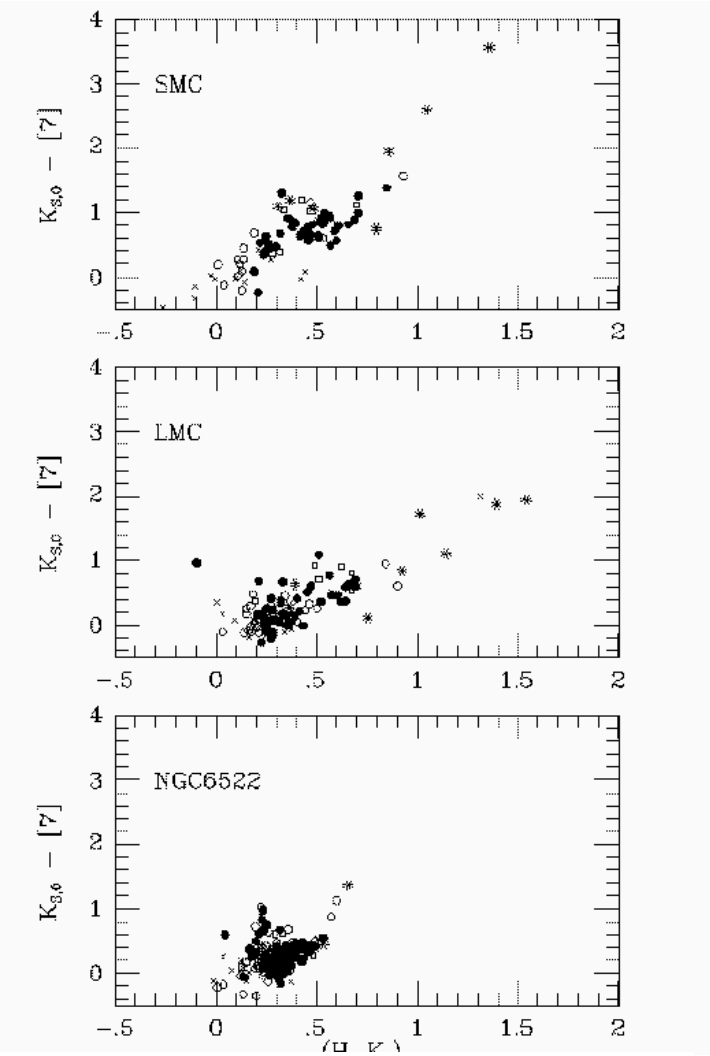


Fig. 12. $(K_{S,0} - [7])$ vs $(H - K_S)_0$ colour-colour diagrams. Note the redward extension in both colours mainly caused by the Magellanic Cloud Miras.

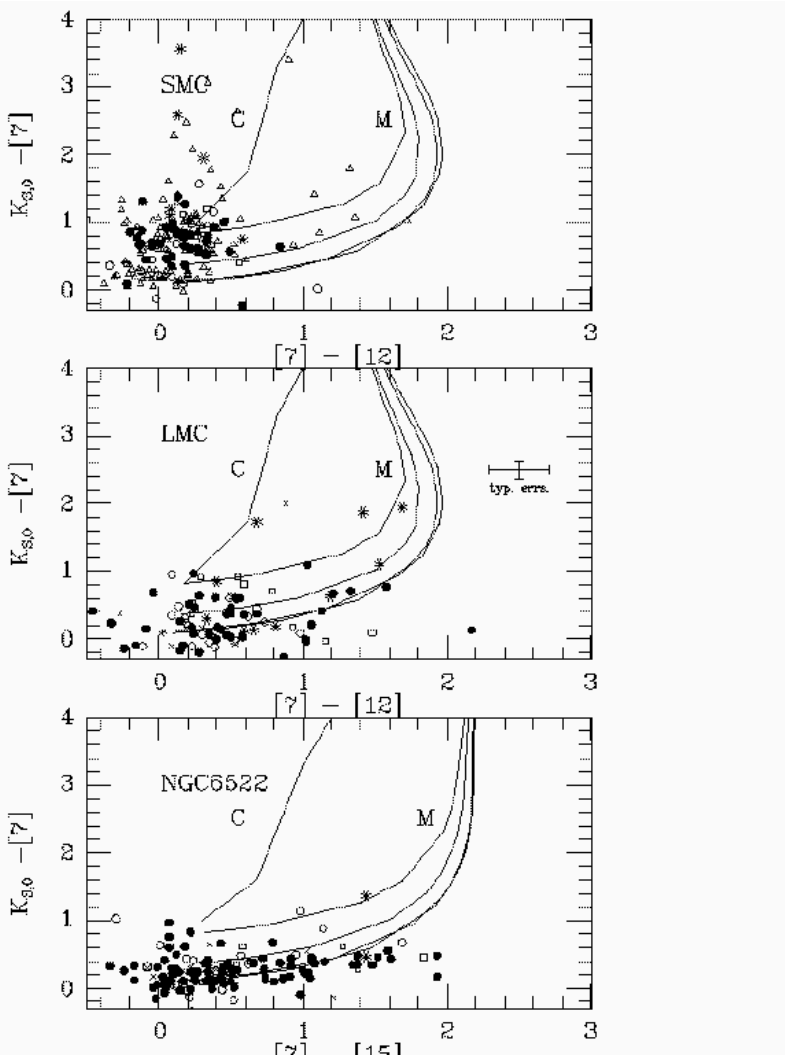


Fig. 13. $K_{S,0} - [7]$ vs. [7] - [12/15] diagram. Also shown are the colours of C, M3, M5, M8 and M10 stars with increasing circumstellar shells, according to the models of Groenewegen (see Loup et al. (2004), in preparation). The approximate locus of carbon stars is shown by the single line to the left and the O-rich models are given as four curved lines, with late types to the right. This diagram distinguishes clearly between (thick) C- and O-rich circumstellar shells. The SMC data have been augmented with some extra stars from Cioni et al. (2003) that fall outside the areas in Table 2 (triangles).

the two Magellanic Cloud fields. There is a clump of variables around $(H - K_S)_0 = 0.3$, $K_{S,0} - [7] = 0.2$ in the NGC 6522 and LMC fields. However, this area is blank in the SMC. This effect is probably due to a lack of ordinary M-type variables in the SMC sample relative to the other two fields, caused by its lower metallicity and increased prevalence of C stars. It will be seen later that very red $(H - K_S)_0$ colours in Mira variables are not necessarily associated with C-richness.

7.3.2. $(K - [7])$ vs $([7] - [12/15])$

The hybrid $K_{S,0} - [7]$ vs. [7] - [12/15] colour-colour diagram (fig. 13) yields the clearest separation between O-rich and C-rich variables. Groenewegen (see Loup et al. (2004), in preparation) has modelled the development of carbon-rich shells for late-type stars as a function of their optical thickness. The carbon models use a simple blackbody underlying spectrum, modified to take into account the 3.1 μm hydrocarbon feature, and the dust is composed of SiC and amorphous C. The M-type models (see Loup et al. (2004), in preparation) combine more realistic central star models from Fluks et al. (1994) with silicate shells.

The LMC Mira-like variables are predominantly of M type and thus O-rich, although there is one probable C Mira. As expected, there are no stars along the C locus in the NGC6522 field.

The SMC sample is concentrated towards the blue end of the range in [7] - [15]. This is mainly the result of the predominance of C-rich stars. The C-type Mira-like variables stand out

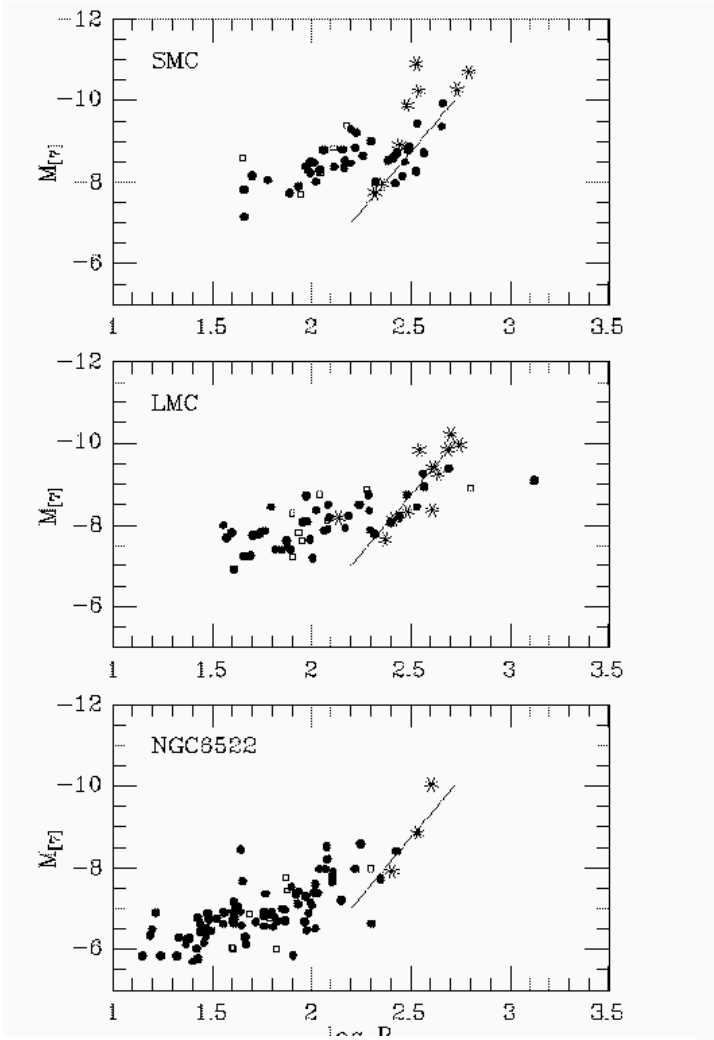


Fig. 14. Absolute 7μm magnitude vs log P. A line has been fitted to the LMC Miras and reproduced at the same position on the other two diagrams.

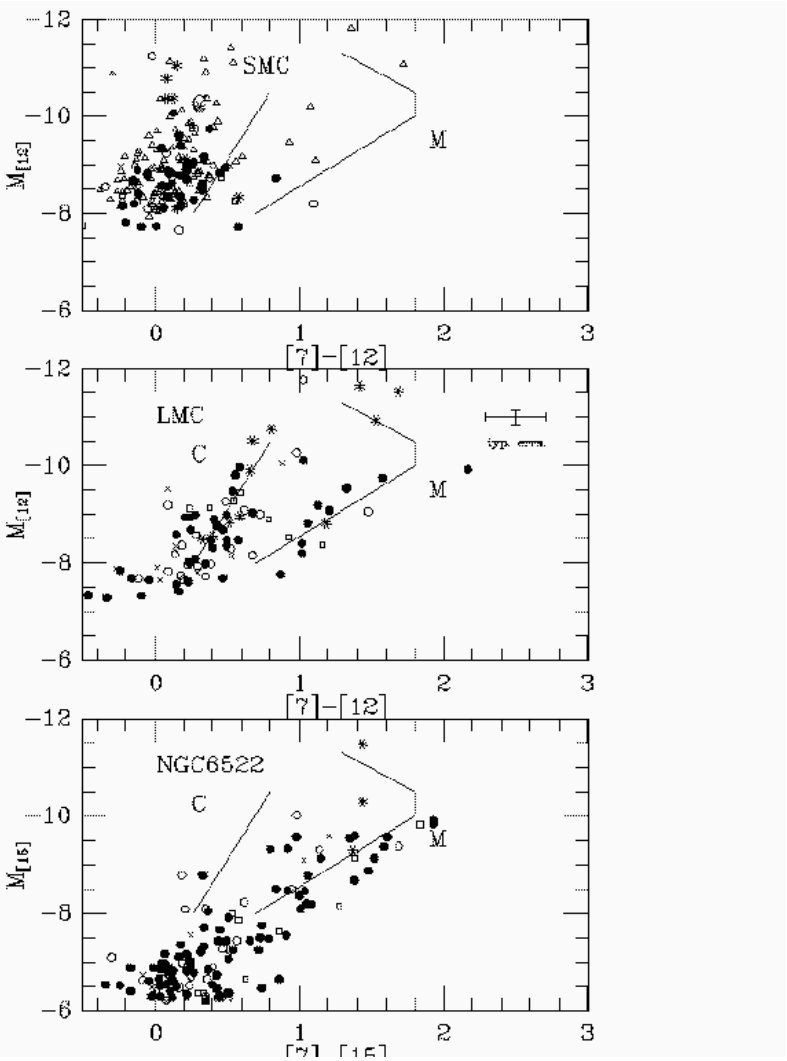


Fig. 15. $M_{[12/15]}$ vs. [7] - [12/15] diagram. It is again noticeable that the variables with developed shells are well separated into C-rich and O-rich sequences. The straight line shows the approximate location of C-rich objects and the kinked line shows the general trend for M-type objects, based on the semi-empirical models discussed in the text. The SMC data have been augmented with some extra stars from Cioni et al. (2003) that fall outside the areas in Table 2 (triangles).

from the locus of C-star models but if K_S mags from DENIS are used, the discrepancy is somewhat reduced. It is believed that their extreme positions are the result of their variability and the times of measurement, besides some contributions from the measurement errors. In order to reduce the effects of small-number statistics, data from the larger area described by Cioni et al. (2003) have also been included.

7.4. Period-$M_{[7]}$ relation

There is a strong suggestion that the period-magnitude relations persist at 7μm (fig. 14). Only the Mira relation is really clear because of the higher photometric errors associated with the ISO measurements.

The stars on the shorter-period sequences disappear as one goes from the NGC 6522 field to the SMC because of the ISO sensitivity limits.

This diagram shows that the 7μm zero points of the Magellanic Clouds are in agreement, though the SMC points could be too high by up to 0.4 mag.

7.4.1. Mid-IR colour-magnitude diagram

In the mid-IR colour-magnitude diagram (fig. 15), because of the different filters, the NGC 6522 and Magellanic field data may not be strictly comparable. The approximate positions of the semi-empirical models discussed previously are shown by a straight line for C-rich stars and by a kinked one for O-rich stars. The shape of the latter line depends only marginally (in relation to the probable errors) on spectral type but can be

moved vertically depending on luminosity. The fundamental chemical differences between the three fields are shown well by these diagrams also.

As a circumstellar shell develops, the M stars at first show redder [7] – [12] colours, in relation to $M_{[12]}$ or $K_{S,0} - [7]$, than the carbon stars, which causes them to follow separate paths in the corresponding diagrams. However, as a thick oxygen-rich shell develops, the [7] – [12] colour ultimately decreases somewhat. The optical thickness at 7μm is probably still developing with increasing dust quantity even as it becomes optically thick at 12μm. The 9.7μm silicate dust feature also absorbs some of the flux in the [12] band under these conditions.

8. Mass-loss

The photospheric radiation at the longest wavelengths (12 or 15μm) can be estimated by assuming that the K fluxes are little affected by circumstellar shells and extrapolating them as Rayleigh-Jeans tails. The existence of the tight K–log$P$ relation for both C- and O-rich stars suggests that K is likely to be almost purely photospheric.

The absolute monochromatic luminosity presumed to arise from dust emission in circumstellar shells is plotted as a function of period in fig 16. The mass-loss levels appear to be similar in spite of the metallicity differences. All fields seem to show some stars with significant mass-loss, beyond $P \sim 100$d. The double-period stars also seem to stand out slightly as more likely to show an excess than variables of similar short period. This is true even for presumably M stars in the NGC 6522 field of the Galaxy. These diagrams will be affected strongly by zero-point errors in the long-wavelength photometry.

9. Conclusions

The three fields we have examined show various similarities and differences. Examining their near infrared colours and magnitudes we see that the level of the RGB tip, $M_{K_0}^{\rm Tip}$ and the $J - K_S$ colour at a defined M_{K_S} (– 5.5) are sensitive to metallicity as expected from galactic globular cluster studies. Near the tip of the AGB the relative numbers of luminous stars, often showing red $J - K_S$ colours, increases towards the low-metallicity fields.

The variable star content of the fields also shows marked differences. Although the same variability classes are present in all three fields, the proportion of stars that are variable, as well as their amplitudes, decreases towards lower metallicity. The period-luminosity loci in the K, log$P$ diagram are also populated in different ways in the three fields.

The mid-IR observations are affected by the sensitivity limit of ISO and the tendency towards larger relative numbers of luminous stars with low-metallicity. The colour-colour and colour-magnitude diagrams can be used to differentiate between oxygen- and carbon-rich stars with developed circumstellar shells. The rates of mass-loss, as judged by the excess fluxes at long wavelength, appear to be similar for the stars in each field.

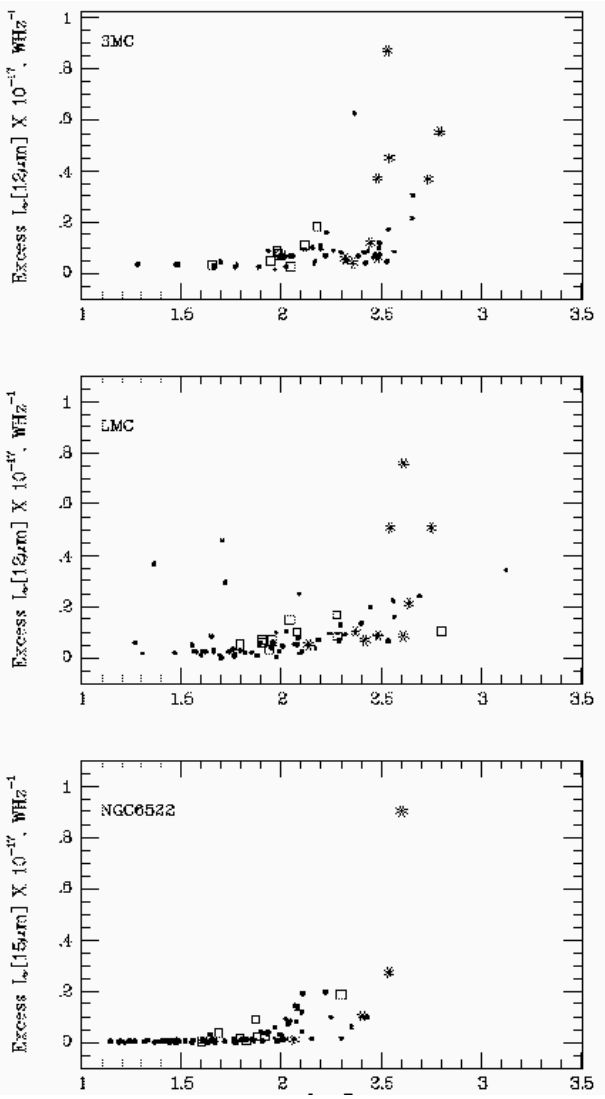


Fig. 16. Absolute monochromatic luminosities of the excess radiation presumed to arise from dust formed during mass-loss, at the wavelengths indicated, above the expected photospheric contribution, assuming that the K flux is all photospheric. Note the general similarity of mass-loss levels (assumed to be affected only moderately by the difference between the 12 and 15μm filter wavelengths). The outlying semi-regular variable points in the LMC fields are attributable to higher than usual errors in the photometry.

10. Acknowledgments

ISG thanks the Institut d'Astrophysique de Paris for their hospitality during part of this work. This visit was supported by the CNRS-NRF agreement. He also thanks the Visitor Programme at the European Southern Observatory for support during a visit of one month.

MS is supported by the APART programme of the Austrian Academy of Science and visited the South African Astronomical Observatory for two weeks under the CNRS-NRF agreement.

Cecile Loup (Institut d'Astrophysique de Paris), and Martin Groenewegen (Institute of astronomy, Katholieke Universiteit, Leuven) are thanked for discussion and information.

This paper utilizes public domain data originally obtained by the MACHO Project, whose work was performed under the joint auspices of the U.S. Department of Energy, National Nuclear Security Administration by the University of California, Lawrence Livermore National Laboratory under contract No. W-7405-Eng-48, the National Science Foundation through the Center for Particle Astrophysics of the University of California under cooperative agreement AST-8809616, and the Mount Stromlo and Siding Spring Observatory, part of the Australian National University.

This publication makes use of data products from the Two-Micron All-Sky Survey, which is a joint project of the University of Massachusetts and the Infrared Processing and Analysis Center, funded by the National Aeronautics and Space ASdministration and the national Science Foundation (USA).

References

Alard, C., Blommaert, J.A.D.L., Cesarsky, C., 2001, ApJ 552, 289
Bessell, M.S., Scholz, M., Wood, P.R., 1996, A&A 307, 481
Blanco V.M., 1986, AJ 91, 290
Cioni M.R., van der Marel R.P., Loup C., et al., 2000, A&A 359, 601
Cioni M.R., Marquette J.-B., Loup C., et al., 2001, A&A 377, 945
Cioni M.R., Blommaert J.A.D.L., Groenewegen M.A.T. et al., 2003, A&A 406, 51
Cioni M.R., Habing H.J., 2003, A&A 402, 133
Feast M.W., Glass I.S., Whitelock P.A., Catchpole R.M., 1989, MNRAS 241, 375
Feast M.W., 1989, in The World of Galaxies, eds Corwin, H.G., Bottinelli, L., p 118
Ferraro F.R., Montegrifo P., Origlia L., Fusi-Pecci F. 2000 AJ, 119, 1282
Fluks M.A., Plez B., The P.S., de Winter D., Westerlund B.E., Steenman H.C., 1994, A&AS, 105, 311
Frogel J.A., Whitelock P.A., 1998, AJ 116, 754
Girardi L., Bressan A., Bertelli G., Chiosi C., 2000, A&AS 141, 371
Glass I.S., Catchpole R.M., Feast M.W., Whitelock P.A., Reid I.N., in *Late Stages of Stellar Evolution*, 51–54. S. Kwok & S.R. Pottasch (eds.), Reidel Dordrecht, 1987.
Glass I.S., Whitelock, P.A., Catchpole, R.M., Feast, M.W., 1995, MNRAS 273, 383
Glass I.S., 1999, in "Handbook of Infrared Astronomy", Cambridge University Press
Glass I.S., Ganesh S., Alard C., et al., 1999, MNRAS 308, 127
Glass, I.S., Schultheis, M., 2002, MNRAS 337, 519
Glass I.S., Schultheis M., 2003, MNRAS 345, 39
Glass I.S., Lloyd Evans T., 2003, MNRAS 343, 57
Glass I.S., Lloyd Evans T., 1981, Nature, 291, 303
Groenewegen M.A.T., A&A (accetped); astro-ph/0404561
Ita Y. et al. 2002 MNRAS 337, L31
Ita Y., Tanabé T., Matsunaga N., et al., 2004, MNRAS 347, 720
Jeong K.S., Winters J.M., Le Bertre T., et al., 2002, in "Mass-losing Pulsating stars and their Circumstellar Matter", eds. Y. Nakada, M. Honma and M.Sekiin
Kiss L.L., Bedding T.R., 2003, MNRAS, 343, L79
Kiss L.L., Bedding T.R., 2004, MNRAS, 347, L83
Lebzelter T., Schultheis M., Melchior A.L., 2002, A&A 393, 573
Lloyd Evans T., 1976, MNRAS, 174, 169
Lloyd Evans T., Glass I.S., Catchpole R.M., 1988, MNRAS 231, 773
Nikolaev S., Weinberg M.D., 2000, ApJ 542, 804
Ojha, D.K., Omont, A., Schuller, F., et al., 2003, A&A 403, 141
Omont A., Gilmore G.F., Alard C., et al., 2003, A&A 403, 975
Reid M.J., Goldston J.E., 2002, ApJ 568, 931
Schuller, F., Ganesh, S., Messineo, M., et al., 2003, A&A 403, 955
Schultheis M., Lançon A., Omont A., et al., 2003, A&A 405, 531
Terndrup D.M., Frogel J.A., Whitford A.E., 1990, ApJ, 357, 453
Tiede, G.P., Frogel, J.A., Terndrup, D.M., 1996, AJ 110, 2788
Wood, P.R., Alcock C., Allsman R.A., et al., 1999, in LeBertre T., Lebre A., Waelkens C., eds, Proc IAU Symp. 191, Asymptotic Giant Stars, Astron. Soc. Pac., San Franscisco, p. 151
Wood, P.R., 2000, PASA, 17, 18
Wray J.J., Eyler L., Paczynski B., 2004, MNRAS 349, 1059